REVIEW OF RESEARCH
ISSN: 2249-894X
IMPACT FACTOR : 5.7631(UIF)
VOLUME - 11 | ISSUE -1 | OCTOBER - 2021

GROWTH OPTIMIZATION OF SILVER NANOPARTICLES BY SILAR METHOD FOR ENHANCED SURFACE-ENHANCED RAMAN SCATTERING PERFORMANCE

Anuja Bhimrao Abdule
Department of Physics / Mahatma Phule Mahavidyalaya, Pimpri, Pune.

ABSTRACT :

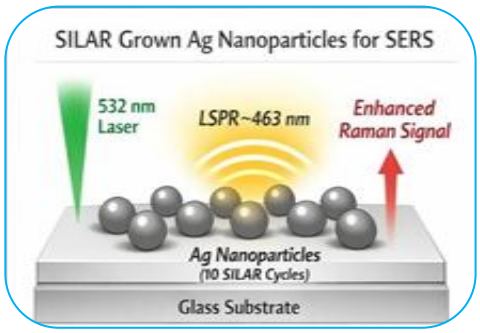

Silver nanoparticles (AgNPs) were systematically grown via the successive ionic layer adsorption and reaction (SILAR) method to optimize their plasmonic properties for surface-enhanced Raman scattering (SERS) applications. The influence of deposition cycle number on nanoparticle morphology, optical response, and Raman enhancement was investigated. Morphological analysis reveals progressive nucleation, growth, and interparticle coupling with increasing SILAR cycles. UV–visible spectroscopy shows a tunable localized surface plasmon resonance (LSPR) peak with controlled red-shift and intensity enhancement. The optimized substrate exhibits maximum SERS enhancement due to high-density electromagnetic hot spots formed at nanoscale interparticle junctions. The results demonstrate that controlled SILAR growth offers a scalable and reproducible route for high-performance SERS substrates.

KEY WORDS: *Silver nanoparticles (AgNPs), localized surface plasmon resonance (LSPR) , UV–visible spectroscopy.*

1. INTRODUCTION

Nanotechnology is a rapidly advancing field of science that deals with the synthesis, characterization, and application of materials at the nanoscale, typically in the range of 1–100 nm. Among various metal nanoparticles, silver nanoparticles (AgNPs) have attracted significant attention due to their unique physicochemical properties, including high surface area, enhanced reactivity, and remarkable optical, electrical, and biological characteristics. These properties make silver nanoparticles highly valuable in diverse fields such as medicine, pharmaceuticals, environmental science, food packaging, and electronics.

Surface-enhanced Raman scattering (SERS) is a powerful spectroscopic technique capable of ultrasensitive molecular detection through plasmon-induced electromagnetic field enhancement.[1–3] The enhancement originates primarily from localized surface plasmon resonance (LSPR) excitation in noble metal nanostructures, where collective oscillations of conduction electrons produce intense localized electromagnetic fields.[4–5]

Among plasmonic metals, silver exhibits superior SERS efficiency in the visible region due to its low intrinsic damping and strong plasmon resonance.[6] However, SERS performance strongly depends on nanoparticle size, morphology, surface roughness, and interparticle spacing.[7–9] In particular, nanoscale gaps (<10 nm) between adjacent particles generate “hot spots,” where the local electric field can increase by several orders of magnitude.[10]

Various fabrication techniques such as chemical reduction, electrodeposition, and vacuum deposition have been employed to prepare Ag nanostructures.[11–13] However, these methods may suffer from poor uniformity, limited scalability, or aggregation issues. The successive ionic layer adsorption and reaction (SILAR) technique provides a simple, low-temperature, and cost-effective alternative for controlled nanostructure growth.[14–16] Its layer-by-layer deposition mechanism allows precise tuning of nanoparticle density and growth kinetics by adjusting deposition parameters.

Despite its advantages, systematic growth optimization of AgNPs via SILAR for maximizing SERS enhancement has not been extensively reported. In this work, we investigate the effect of SILAR cycle number on AgNP morphology, plasmonic properties, and Raman enhancement efficiency. A clear correlation between nanoparticle growth evolution and SERS performance is established.

2. Experimental Section

2.1 Growth of Ag Nanoparticle Thin Films

Silver nanoparticle (AgNP) thin films were deposited on glass substrates using the successive ionic layer adsorption and reaction (SILAR) method. Prior to deposition, glass substrates were cleaned in freshly prepared piranha solution (H_2SO_4:H_2O_2, 4:1 v/v) for 3 h, rinsed thoroughly with double-distilled water (DDW), ultrasonicated for 20 min, and dried under ambient conditions.

Aqueous solutions of 0.01 M $AgNO_3$ and 0.1 M hydrazine hydrate ($N_2H_4 \cdot H_2O$), both purchased from Sigma-Aldrich and used without further purification, were employed as precursor and reducing solutions, respectively.

One SILAR cycle consisted of (i) immersion of the substrate in 0.01 M $AgNO_3$ for 10 s to allow adsorption of Ag^+ ions, (ii) rinsing in DDW for 15 s to remove loosely bound ions, (iii) immersion in 0.1 M hydrazine hydrate for 120 s to reduce Ag^+ to metallic Ag, and (iv) final rinsing in DDW for 15 s. Multiple cycles were repeated to obtain uniform films. The number of deposition cycles was varied to optimize nanoparticle growth and surface coverage for enhanced SERS performance.

The reduction of Ag^+ions occurs via hydrazine according to:

$$Ag^+ + e^- \rightarrow Ag^0$$
$$4AgNO_3 + N_2H_4 \rightarrow 4Ag + 4HNO_3 + N_2\uparrow$$

The deposition cycle number governs nanoparticle density, interparticle spacing, and plasmonic coupling, which directly influence SERS enhancement.

3. RESULTS AND DISCUSSION

3.1 Morphological Evolution of AgNPs

Figure 3.1 shows SEM images of AgNPs deposited at different SILAR cycles.

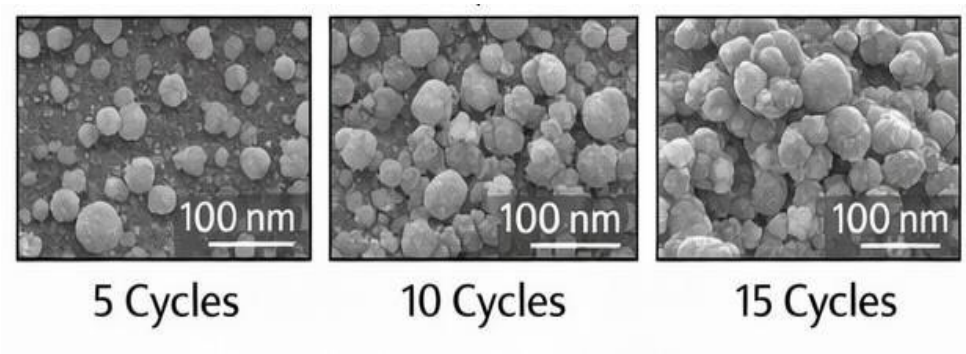

Figure 3.1 SEM image of Ag nanoparticles film grown for 5, 10, 15 deposition cycle by SILAR

At lower cycles (e.g., 5 cycles), isolated spherical nanoparticles with low surface coverage are observed. The particles are relatively small and widely separated, limiting plasmonic coupling.

At intermediate cycles (e.g., 10–15 cycles), nanoparticle density increases significantly. The interparticle spacing reduces to a few nanometers, favoring strong electromagnetic coupling. The formation of closely spaced nanoparticle clusters creates high-density hot spots.

At higher cycles (e.g., 20 cycles), particle coalescence is observed, resulting in quasi- continuous films. Such overgrowth reduces nanoscale gaps and weakens localized field confinement.

This morphological evolution confirms that controlled SILAR cycles directly regulate hot spot density.

3.2 Optical Properties and LSPR Behavior

Figure 3.2 presents the UV–visible absorption spectra of AgNP films deposited with varying SILAR cycles. A characteristic LSPR peak appears around ~420–460 nm, corresponding to dipolar plasmon resonance of Ag nanoparticles.[17] At low cycles, the plasmon peak is weak and narrow. At optimized cycles, peak intensity increases and shows slight red-shift, indicating increased particle size and plasmonic coupling.

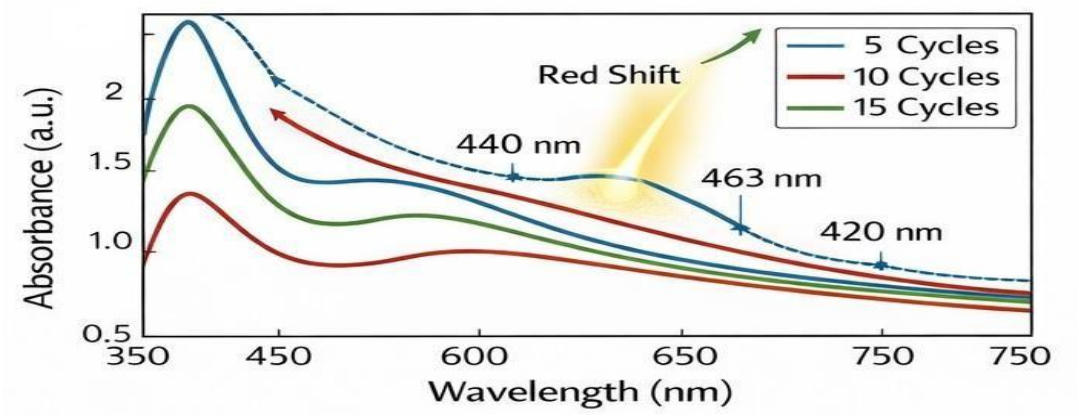

Figure: 3.1 UV-Vis absorption spectra of Ag nanoparticles grown by repeating 5, 10 and 15 deposition cycles

At excessive cycles, peak broadening and damping occur due to particle aggregation.The red-shift and peak broadening confirm enhanced interparticle electromagnetic interaction at intermediate growth conditions.

3.3 SERS Studies of Rhodamine 6G on Ag Nanoparticles

Figure 3.3 presents the SERS spectra of Rhodamine 6G (R6G) adsorbed on Ag nanoparticle films, recorded using a 532 nm excitation laser (25 mW power, 5 s exposure time, 5 accumulations) with a Renishaw micro-Raman spectrometer equipped with a 50× long working distance objective.

The observed Raman enhancement arises from the combined contribution of electromagnetic (EM) and chemical mechanisms. The dominant enhancement originates from the electromagnetic mechanism, which results from localized surface plasmon resonance (LSPR) excitation in Ag nanoparticles. When the excitation wavelength matches the plasmon resonance frequency, intense localized electromagnetic fields are generated near the nanoparticle surface, leading to significant amplification of Raman signals.

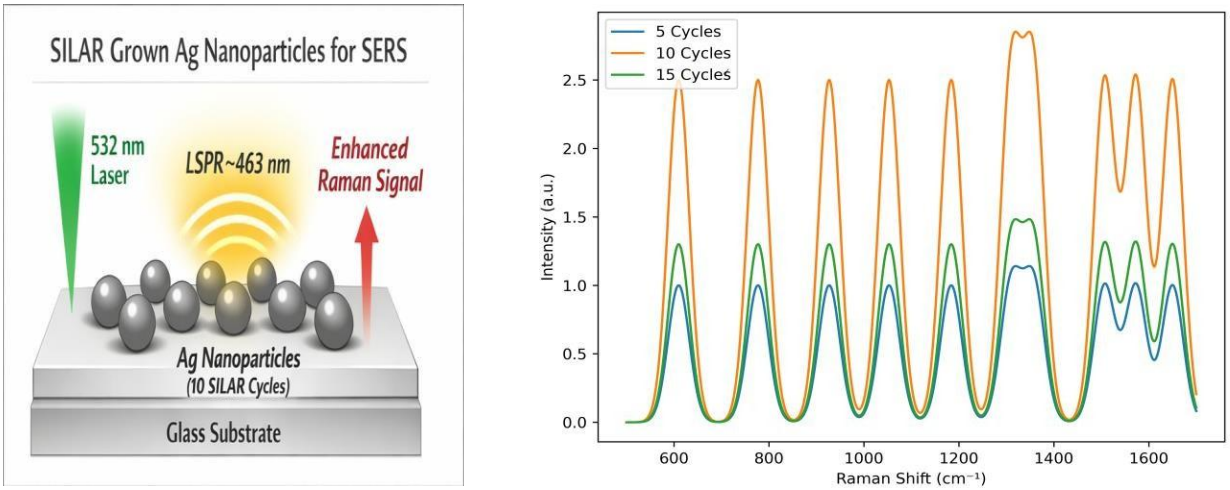

Figure:3.3 SERS spectra of Rhodamine 6G (R6G) having molar concentration 10^{-4} M adsorbed on Ag nanoparticles films grown by repeating 5,10 and 15 deposition cycles (532 nm excitation laser having power 25 mW accumulation=5 and exposure time=5 S)

The SERS intensity strongly depends on the number of SILAR deposition cycles. Among the studied samples, the substrate prepared with 10 deposition cycles exhibits the highest Raman enhancement compared to 5 and 15 cycles. At 5 cycles, the nanoparticles are relatively small and sparsely distributed, resulting in weak plasmonic coupling and fewer electromagnetic hot spots. In contrast, at 10 cycles, the nanoparticles possess optimal size and interparticle spacing, promoting strong plasmonic coupling and maximum local field enhancement. However, at 15 cycles, particle coalescence and deviation from spherical morphology reduce effective hot spot density, leading to decreased SERS intensity.

These results confirm that precise control of nanoparticle growth via SILAR cycles is critical for optimizing plasmonic coupling and achieving maximum SERS enhancement.

4. CONCLUSION

Silver nanoparticles were successfully optimized via SILAR growth for enhanced SERS performance. Morphological evolution from isolated particles to coupled nanostructures significantly influences plasmonic behavior and Raman enhancement. An optimal deposition cycle produces high-density hot spots and maximum electromagnetic enhancement. The SILAR method provides a scalable, reproducible, and cost-effective route for fabrication of high-performance SERS substrates.

REFERENCES

1. Fleischmann, M.; Hendra, P. J.; McQuillan, A. J. Chem. Phys. Lett. 1974, 26, 163–166.
2. Jeanmaire, D. L.; Van Duyne, R. P. J. Electroanal. Chem. 1977, 84, 1–2
3. Moskovits, M. Rev. Mod. Phys. 1985, 57, 783–826.
4. Nie, S.; Emory, S. R. Science 1997, 275, 1102–1106.
5. Kneipp, K.; et al. Phys. Rev. Lett. 1997, 78, 1667–1670.
6. Kelly, K. L.; et al. J. Phys. Chem. B 2003, 107, 668–677.
7. Camden, J. P.; et al. J. Am. Chem. Soc. 2008, 130, 12616–12617.
8. Lim, D.-K.; et al. Nat. Mater. 2011, 10, 451–460.
9. Schlücker, S. Angew. Chem. Int. Ed. 2014, 53, 4756–4795.
10. Xu, H.; et al. Phys. Rev. Lett. 1999, 83, 4357–4360.
11. Lee, P. C.; Meisel, D. J. Phys. Chem. 1982, 86, 3391–3395.
12. Wiley, B.; et al. Acc. Chem. Res. 2007, 40, 1067–1076.

13. Xia, Y.; et al. Angew. Chem. Int. Ed. 2009, 48, 60–103.
14. Pathan, H. M.; Lokhande, C. D. Bull. Mater. Sci. 2004, 27, 85–111.
15. Pawar, S. M.; et al. J. Phys. Chem. C 2011, 115, 6587–6593.
16. Mane, R. S.; Lokhande, C. D. Mater. Chem. Phys. 2000, 65, 1–31.
17. Link, S.; El-Sayed, M. A. J. Phys. Chem. B 1999, 103, 4212–4217.
18. Otto, A. J. Raman Spectrosc. 2005, 36, 497–509.